AND gate based on two-photon absorption in semiconductor optical amplifier

Amer Kotb[1,2]*
1. *Department of Physics, Fayoum University, Fayoum 63514, Egypt*
2. *Department of Physics, College of Science, Northern Borders University, Arar 1321, KSA*

(Received 28 December 2012)

An all-optical logic AND gate based on two-photon absorption (TPA) in semiconductor optical amplifier (SOA) is simulated. By solving the rate equations of SOA in the form of a Mach-Zehnder interferometer (MZI), the performance of AND gate is numerically investigated. The model takes the effects of amplified spontaneous emission (ASE) and pulse energy on the system's quality factor (Q-factor) into account. Results show that the all-optical AND gate based on TPA in SOA-MZI based structure is feasible at 250 Gbit/s with a proper Q-factor.
Document code: A **Article ID:** 1673-1905(2013)03-0181-4
DOI 10.1007/s11801-013-2418-7

In future high-speed communication systems, optical logic gates are expected to play an important role in switching, signal regeneration, addressing, header recognition, data encoding and encryption, etc. In recent years, optical logic gates based on several different schemes have been demonstrated and reported, including that based on dual-semiconductor-optical-amplifier (SOA) Mach-Zehnder interferometer (MZI)[1,2], semiconductor laser amplifier loop mirror (SLALM)[3], ultrafast nonlinear interferometer (UNI)[4], four-wave mixing (FWM) process in SOA[5], and cross-gain modulation (XGM) or cross-phase modulation (XPM) in nonlinear devices[6]. Among these schemes, the SOA based on MZI has the advantages of being relatively stable, simple and compact. All-optical logic gate based on two-photon absorption (TPA) in SOAs was presented[7,8]. All-optical logic performance and high speed of quantum-dot (QD) SOA based devices were studied[9,10].

In this paper, an all-optical logic AND operation based on TPA of pump beams is modeled. The proposed device is an MZI, each arm of which has an SOA. The simulation is performed under a repetition rate of ~ 250 Gbit/s. Effects of amplified spontaneous emission (ASE) and pulse energy on the system's quality factor (Q-factor) are studied. In Refs.[9] and [10], the effects of ASE on the output gates were not taken into account. Effect of ASE on bulk SOAs-based all-optical logic gate is modeled[11-13]. When TPA of a high-intensity pump beam takes place in an SOA, there is an associated fast phase change in the weak probe signal. The primary noise in this calculation which lowers the Q-factor in the absence of ASE noise is pattern effect resulting from long recovery time of gain and gain-induced phase change. The ASE causes additional output noise through spontaneous-spontaneous beat noise and signal-spontaneous beat noise. In addition, if one wants to measure the error rate of the gate output, the dark current of the photodiode, shot noise and thermal noise need to be considered. The ASE related noise depends on the spontaneous emission factor (N_{SP}) of the amplifier.

The new element is the phase change (Φ_{TPA}) due to TPA has a fast component, which is given by[7,8]:

$$\Phi_{TPA} = -0.5\beta\alpha_{TPA}S(t)\,, \tag{1}$$

where β is the TPA parameter, α_{TPA} is the linewidth enhancement factor for TPA, and $S(t)$ is the optical pump pulse energy. The negative sign represents the observation that the TPA-induced phase change is in an opposite direction from that for gain-induced phase change. The experimentally derived α_{TPA} is ~ 4–5, and the quantity β is ~ 20–35 cm/GW[7, 8]. For an SOA with a cross-section of 5×10^{-9} cm^2, the pulse width is 0.5 ps at 250 Gbit/s.

SOAs incorporated into MZI are used for wavelength conversion and demultiplexing high-speed time division multiplexed (TDM) optical signals. The schematic diagram of an MZI with integrated SOA for AND operation is shown in Fig.1, where BPF means band-pass filter.

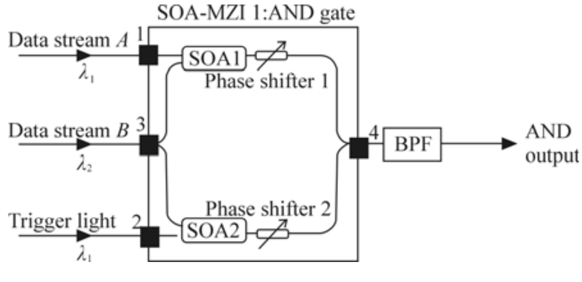

Fig.1 Schematic diagram of the MZI with integrated SOA for AND operation

* E-mail: amer_22003@yahoo.com

The operation of SOA-MZI can be studied using a rate equation model. The carrier heating results from a thermalization of carriers in the entire energy band following the pulse. This is a fast process occurring in time scale from 0.1 ps to 0.7 ps. The injected pulse reduces the gain at the photon energy of this pulse, i.e., in the gain spectrum it burns a hole. The process is known as spectral hole burning. By taking both carrier heating and spectral hole-burning effects into consideration, the time-dependent gain for each SOA is given by[13]:

$$\frac{\mathrm{d}h(t)}{\mathrm{d}t}=\frac{h_0-h(t)}{\tau_c}-\{\exp[h(t)+h_{\mathrm{CH}}(t)+h_{\mathrm{SHB}}(t)]-1\}S(t,0), \tag{2}$$

$$\frac{\mathrm{d}h_{\mathrm{CH}}(t)}{\mathrm{d}t}=-\frac{h_{\mathrm{CH}}(t)}{\tau_{\mathrm{CH}}}-\frac{\varepsilon_{\mathrm{CH}}}{\tau_{\mathrm{CH}}}\{\exp[h(t)+h_{\mathrm{CH}}(t)+h_{\mathrm{SHB}}(t)]-1\}S(t,0), \tag{3}$$

$$\frac{\mathrm{d}h_{\mathrm{SHB}}(t)}{\mathrm{d}t}=-\frac{h_{\mathrm{SHB}}(t)}{\tau_{\mathrm{SHB}}}-\frac{\varepsilon_{\mathrm{SHB}}}{\tau_{\mathrm{SHB}}}\{\exp[h(t)+h_{\mathrm{CH}}(t)+h_{\mathrm{SHB}}(t)]-1\}S(t,0)-\frac{\mathrm{d}h(t)}{\mathrm{d}t}-\frac{\mathrm{d}h_{\mathrm{CH}}(t)}{\mathrm{d}t}. \tag{4}$$

The total gain $G(t)$ is given by

$$G(t,z)=\exp[h(t)+h_{\mathrm{CH}}(t)+h_{\mathrm{SHB}}(t)], \tag{5}$$

where $h(t)$ is an integral of optical gain per unit length over the length of SOA, and the total equals the sum of h, h_{CH} and h_{SHB}. τ_c is the carrier lifetime, and $G_0=\exp(h_0)$ is the unsaturated power gain. $S(t, 0)$ is the instantaneous input optical intensity inside the SOA, and h, h_{CH} and h_{SHB} are the h-factor values for carrier recombination, carrier heating and spectral hole burning, respectively. τ_{CH} and τ_{SHB} are the temperature relaxation rate and the carrier-carrier scattering rate, respectively. $\varepsilon_{\mathrm{CH}}$ and $\varepsilon_{\mathrm{SHB}}$ are the nonlinear gain suppression factors due to carrier heating and spectral hole burning, respectively.

For the used β of 30 cm/GW, the change of intensity due to TPA is low, hence it is neglected in this model. The carrier density induced phase change is given by[9,10]:

$$\Phi(t)=-0.5\,[\alpha h(t)+\alpha_{\mathrm{CH}}h_{\mathrm{CH}}(t)]-0.5\beta\alpha_{\mathrm{TPA}}S(t), \tag{6}$$

where α is the traditional linewidth enhancement factor, α_{CH} is the carrier heating alpha factor, and α_{SHB} is the spectral hole-burning alpha factor.

We assume the data stream pulse to be a Gaussian pulse, i.e.,

$$P_{A,B}(t)=\sum_{n=-\infty}^{n=+\infty}a_{nA,B}\frac{2\sqrt{\ln(2)}\,P_0}{\sqrt{\pi}\,\tau_{\mathrm{FWHM}}}\times\exp\left(-\frac{4\ln(2)(t-nT)^2}{\tau^2_{\mathrm{FWHM}}}\right), \tag{7}$$

where $a_{nA,B}$ represents the nth data in data streams A and B, which equals 1 or 0. P_0 is the input pulse energy, and T is the bit period. τ_{FWHM} is the pulse width (full width at half maximum).

All-optical AND gate employing an SOA has been demonstrated[11,13]. It is important that the gate is stable and compact. In order to realize AND operation, data A at wavelength λ_1 and a delayed version of data A are injected into each of the two SOAs. Data stream B at wavelength λ_2 is injected into both arms as control beam. The phases (phase shifter in Fig.1) in the two arms are set, so that when there is no additional phase shift, the phase difference is π between two arms and the output is zero. The data A and delayed data A produce a phase gate for data B. When $A=0$, this phase gate does not exist, thus the output is 0 for both $B=1$ and $B=0$. When $A=1$ and $B=1$, the phase gate allows the $B=1$ to interfere nondestructively at the output, which results in a non-zero output. Thus this configuration provides a process which gives "1" at output at λ_2 only when both data A and B are "1", which is functionally the same as an all-optical AND gate.

The AND gate operation is analyzed by a numerical solution of the SOA rate equations stated earlier. At the output end of the MZI, the signal outputs with the wavelength of λ_2 from both SOAs interfere, and the AND output intensity is given by:

$$P_{\mathrm{AND}}(t)=\frac{P_B(t)}{4}\{G_1(t)+G_2(t)-2\sqrt{G_1(t)G_2(t)}\times\cos[\Phi_1(t)-\Phi_2(t)]\}, \tag{8}$$

where $P_B(t)$ represents the power of pump signal B before SOAs, $G_{1,2}(t)$ is time-dependent gain of SOA, and $\Phi_{1,2}(t)$ is the phase shift due to SOA and TPA. The SOA parameters used in this simulation are $P_0=0.01$ pJ, $\tau_{\mathrm{FWHM}}=0.5$ ps, $\tau_c=300$ ps, $\tau_{\mathrm{CH}}=0.3$ ps, $\tau_{\mathrm{SHB}}=0.1$ ps, $\varepsilon_{\mathrm{CH}}=\varepsilon_{\mathrm{SHB}}=0.08$ ps, $\alpha=7$, $\alpha_{\mathrm{CH}}=1$, $P_{\mathrm{sat}}=28$ mW, $\beta=30$ cm/GW and $\alpha_{\mathrm{TPA}}=4$. Fig.2(a) illustrates the simulation results of AND gate operation with the patterns of signal A and signal B. The bottom trace shows the AND output after SOA-MZI. Fig.2(b) shows the eye diagram of AND output for pseudo-random data inputs. The primary reason for noise in this calculation which lowers the Q-factor in the absence of ASE noise is pattern effect resulting from long recovery time of gain and gain-induced phase change.

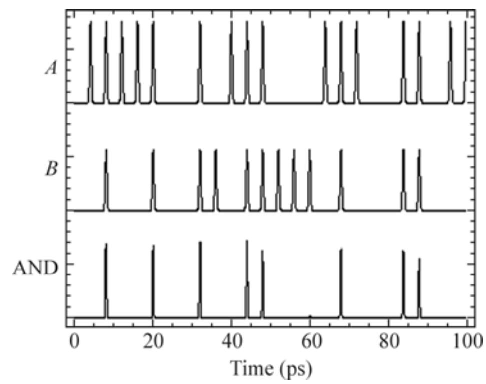

(a)

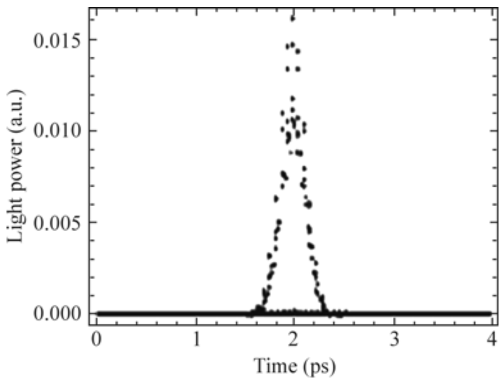

(b)

Fig.2 (a) Simulated results of SOA-MZI for AND output; (b) Eye diagram for AND output

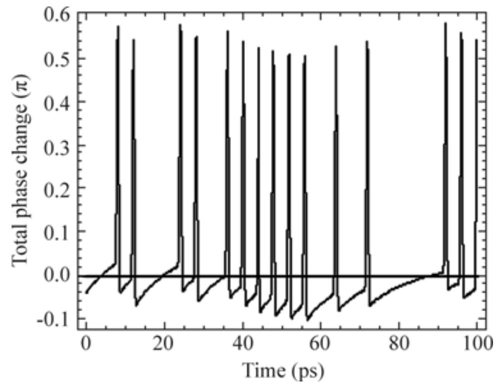

(c)

Fig.3 (a) Phase change due to the gain; (b) Phase change due to TPA; (c) Total phase change

The calculated phase changes as a function of time, which are the phase change due to the gain of SOA-MZI, the phase change due to TPA in SOA-MZI and the total phase for both SOA-MZI and TPA, are shown in Fig.3.

Q-factor of AND output signal is calculated. *Q*-factor gives the information of the optical signal to noise ratio (OSNR) in digital transmission. *Q*-factor is given by $Q = (S_1 - S_0) / (\sigma_1 + \sigma_2)$, where S_1, S_0 are the average intensities of the expected "1"s and "0"s, and σ_1, σ_2 are standard deviations of those intensities. *Q*-factor increases with the decreasing carrier lifetime and drops with the increasing input pulse energy. We have investigated the effect of ASE power. The ASE power is related to N_{SP} by the relation:

$$P_{ASE} = N_{SP}(G-1)\,h\upsilon B_0\,, \quad (9)$$

where G is the maximum gain, h is Plank's constant, υ is the frequency and B_0 is the bandwidth. The ASE noise is added numerically using Eq.(9) on the pattern effect noise to obtain the *Q*-factor. The *Q*-factor versus N_{SP} at 250 Gbit/s for AND output is shown in Fig.4(a). For an ideal amplifier (N_{SP} = 2), the *Q*-factor at 30 dB gain is 10.4 at 250 Gbit/s. The time delay between *A* and its delayed version affects the performance of the AND gate. The calculated *Q*-factor as a function of delay is shown in Fig.4(b). The optimum performance (high *Q*-factor) is achieved for a small range of delay.

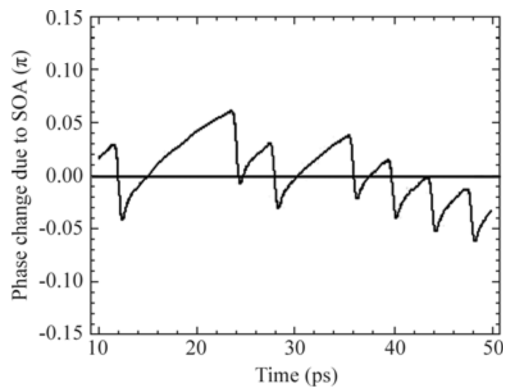

(a)

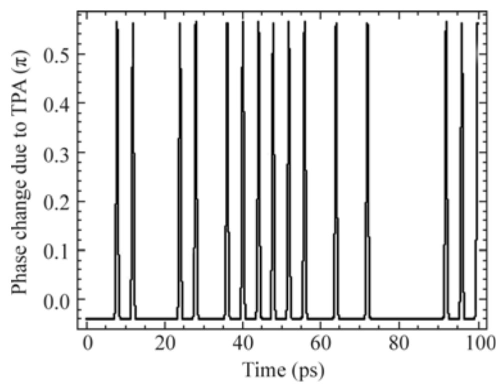

(b)

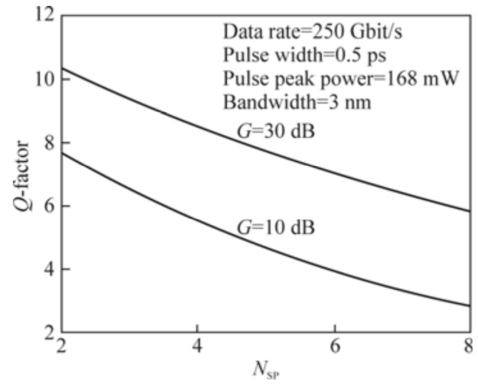

(a)

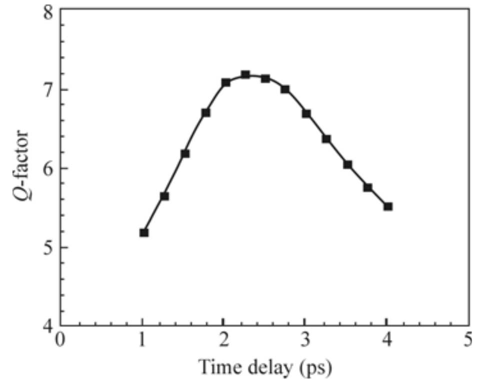

(b)

Fig.4 (a) *Q*-factor versus N_{SP} for AND operation; (b) Calculated *Q*-factor as a function of time delay

To obtain further information on the AND gate performance, the *Q*-factors for different input single-pulse energy values at 250 Gbit/s are calculated as shown in Fig.5. An increase of input pulse energy will make the SOA easier to saturate, which results in a decrease in the *Q*-factor.

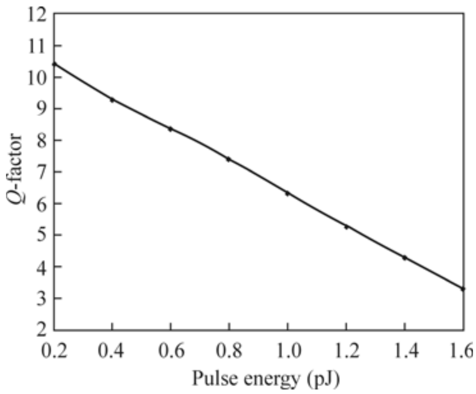

Fig.5 *Q*-factor versus pulse energy

In this paper, we demonstrate an all-optical logic AND gate based on TPA using SOA-MZI. By solving the rate equations of SOA-MZI, we investigate the AND gate performance numerically. Results show that the all-optical AND gate based on TPA in SOA-MZI based structure is feasible at 250 Gbit/s with a proper *Q*-factor. The model takes the effects of ASE and pulse energy on the system's *Q*-factor into account. ASE is calculated as a function of the spontaneous emission factor (N_{SP}). A decrease in quality factor is predicted for high N_{SP}. The effect of ASE can be experimentally verified by adding wideband (a few nanometers wide) optical unmodulated signal to the data and measuring the *Q*-factor as a function of the intensity and bandwidth of this signal. ASE effects are important for the cascaded logic operations.

References

[1] Q. Wang, G. Zhu, H. Chen, J. Jaques, J. Leuthold, A. B. Piccirilli and N. K. Dutta, IEEE J. Quantum Electron **40**, 703 (2004).

[2] J. Y. Kim, J. M. Kang, T. Y. Kim and S. K. Han, Electron. Lett. **42**, 303 (2006).

[3] T. Houbavlis, K. Zoiros, A. Hatziefremidis, H. Avramopoulos, L. Occhi, G. Guekos, S. Hansmann, H. Burkhard and R. Dall'Ara, Electron. Lett. **35**, 1650 (1999).

[4] C. Bintjas, M. Kalyvas, G. Theophilopoulos, T. Stathopoulos, H. Avramopoulos, L. Occhi, L. Schares, G. Guekos, S. Hansmann and R. Dall'Ara, IEEE Photon. Technol. Lett. **12**, 834 (2000).

[5] K. Chan, C. Chan, L. Chen and F. Tong, IEEE Photon. Technol. Lett. **16**, 897 (2004).

[6] Z. Li, Y. Liu, S. Zhang, H. Ju, H. de-Waardt, G. D. Khoe, S. Dorren and D. Lenstra, Electron. Lett. **41**, 1397 (2005).

[7] A. Kotb, S. Ma, Z. Chen, N. K. Dutta and G. Said, Optics Communications **283**, 4707 (2010).

[8] H. Sun, Q. Wang, H. Dong and N. K. Dutta, Microwave and Optical Technology Letters **48**, 29 (2006).

[9] S. Ma, A. Kotb, Z. Chen and N. K. Dutta, Proceeding of SPIE **7750**, 77501L (2010).

[10] S. Ma, Z. Chen, H. Sun and N. K. Dutta, Optics Express **18**, 6417 (2010).

[11] A. Kotb, S. Ma, Z. Chen, N. K. Dutta and G. Said, Optics Communications **284**, 5798 (2011).

[12] A. Kotb and J. Maeda, Optoelectronics Letters **8**, 437 (2012).

[13] Amer Kotb, All-Optical Logic Gates using Semiconductor Optical Amplifiers, Lambert Academic Publishing, Germany, 2012.